Supplemental Material

Generation, characterization, and toxicological assessment of reference ultrafine soot particles with different organic content for air-liquid interface exposures

Anusmita Das, Jana Pantzke, Seongho Jeong, Elena Hartner, Elias J. Zimmermann, Nadine Gawlitta, Svenja Offer, Deeksha Shukla, Anja Huber, Narges Rastak, Arūnas Meščeriakovas, Natalia P. Ivleva, Evelyn Kuhn, Stephanie Binder, Sebastian Oeder, Mathilde Delaval, Thomas Gröger, Hendryk Czech, Olli Sippula, Jürgen Schnelle-Kreis, Sebastiano Di Bucchianico, Martin Sklorz, Ralf Zimmermann*

*Corresponding author: ralf.zimmermann@uni-rostock.de

Table of Contents

Table S1. Column setup of GC×GC-analysis. Columns were purchased from SGE, Australia.

Location	**Phase**	**Length** [m]	**Inner Diameter** [mm]	**Film Thickness** [µm]
Pre-column	BPX5	1.3	0.25	0.25
1st dimension Oven	BPX5	60	0.25	0.25
2nd dimension Oven	BPX50	1.5	0.1	0.1

Table S2. GC oven temperature profile of GC×GC analysis of PM samples. The secondary oven was used with a temperature offset of 5 °C relative to the GC oven temperature. The modulator temperature offset was 15 °C relative to the secondary oven temperature. The modulation time was set to 5 s. Hot pulse time was 1.5 s. Cool time between stages 1.0 s.

T rate [°C min^{-1}]	**T** [°C]	**Hold time** [min]
-	50	5
5	150	-
3	340	15

Table S3. Classification settings. Retention time range and mass spectral filter for each class are summarized in the table below.

Class	**Retention time 1** [s]	**Retention time 2** [s]	**Most prominent m/z**
4-Ring PAHs	4200-4600	4.0-5.2	228, 114; 226
Alk 4-Ring PAHs	4000-4700	3.6-5.0	242, 121
5-& 6-Ring PAHs	4800-5100; 4700-5500; 5300-5600	4.7-6.0; 4.6-6.5; 1.5-3.0	252; 276; 278;
Alk 5-Ring PAHs	4700-5300	4.4-6.0	266, 133
Oxy-PAHs	4100-4700; 4800-5100	4.2-5.4; 4.8-5.4	268, 134

Table S4. Flow settings of inlet system. Helium was used as carrier gas.

Column flow [mL min^{-1}]	**Split flow** [mL min^{-1}]	**t** [s]
1.0	100	90
2.6	0	910
1.0	100	until end of analysis

Table S5. Temperature settings of inlet system.

T rate [°C s^{-1}]	**T** [°C]	**t** [s]
-	40	100
2	300	1600
-	280	until end of analysis

Table S6. Time periods of the different measurement campaigns and assigned groups

Time period of the measurement campaign	Assigned group
July 2021 – August 2021	Group A
May 2022	Group B
August 2022	Group C

Table S7. Comparison of the physical and optical properties of the reference UFPs (UFP-H and UFP-L) produced during three measurement campaigns (Group A, Group B, Group C). The results are shown as mean ± standard deviation of n individual experiments performed in each group. For UFP-H: n= 11 (group A), n= 5 (group B) and n= 5 (group C). For UFP-L: n= 8 (group A), n= 4 (group B) and n= 3 (group C).

	UFP- H			**UFP- L**		
	Group A	Group B	Group C	Group A	Group B	Group C
Mass concentration ($\mu g/m^3$)	110 ± 2	130 ± 7	120 ± 12	90 ± 10	100 ± 1	110 ± 7
PNC ($\#/cm^3$)	49E+04 ± 2E+04	57E+04 ± 4E+04	53E+04 ± 5E+04	52E+04 ± 3E+04	42E+04 ± 10E+04	48E+04 ± 4E+04
GMD_{mob} (nm)	45 ± 1	40 ± 1	40 ± 1	40 ± 1	40 ± 0	40 ± 2
AAE (470/950)	2.0 ± 0.1	1.9 ± 0.1	1.8 ± 0.1	1.7 ± 0.0	1.7 ± 0.0	1.5 ± 0.2
AAE (370/880)	2.0 ± 0.1	2.0 ± 0.1	1.9 ± 0.1	1.7 ± 0.0	1.7 ± 0.0	1.5 ± 0.1
eBC ($\mu g/m^3$)	47 ± 2	60 ± 6	57 ± 2	51 ± 3	67 ± 3	69 ± 3

Table S8. Summary statistics of Welch's ANOVA (along with p-values), the Bonferroni corrected p-values (when p <0.05) and the fold change between the different groups for UFP-H.

	p-value Welch-ANOVA	**p-value Welch-ANOVA <0.05: p-value (Bonferroni) Group A vs Group B**	**fold change Group A / Group B**	**if p-value Welch-ANOVA <0.05: p-value (Bonferroni) A vs C**	**fold change Group A /Group C**	**if p-value Welch-ANOVA <0.05: p-value (Bonferroni) Group B vs Group C**	**fold change Group B / Group C**
Mass concentration	0.0230	0.0130	0.9	0.7050	0.9	1.0000	1.1
PNC	0.0318	0.0550	0.9	0.6040	0.9	0.7420	1.1
GMD_{mob}	0.0001	0.0150	1.0	2.10^{-5}	1.1	0.6660	1.0
AAE (470/950)	0.0423	0.2700	1.0	0.0740	1.1	0.8250	1.0
AAE (370/880)	0.2713	Not applicable	1.0	Not applicable	1.0	Not applicable	1.0
eBC	0.0003	0.0956	0.8	0.0002	0.8	1.0000	1.0

Table S9. Summary statistics of Welch's ANOVA (along with p-values), the Bonferroni corrected p-values (when p <0.05) and the fold change between the different groups for UFP-L.

	p-value Welch-ANOVA	**p-value Welch-ANOVA <0.05: p-value (Bonferroni) Group A vs Group B**	**fold change Group A / Group B**	**if p-value Welch-ANOVA <0.05: p-value (Bonferroni) A vs C**	**fold change Group A /Group C**	**if p-value Welch-ANOVA <0.05: p-value (Bonferroni) Group B vs Group C**	**fold change Group B / Group C**
Mass concentration	0.0377	0.0170	0.9	0.0450	0.8	0.8320	0.9
PNC	0.0025	0.0001	1.2	0.7200	1.1	0.3000	0.9
GMD_{mob}	0.0021	0.0001	0.9	1.0000	1.0	0.3000	1.1
AAE (470/950)	**	1.0000	1.0	0.9100	1.1	0.8100	1.1
AAE (370/880)	0.228	Not applicable	1.0	Not applicable	1.1	Not applicable	1.1
eBC	0.003	0.0002	0.8	0.0037	0.7	1.0000	1.0

**Welch-ANOVA cannot be calculated as one within-group, the standard deviation is zero, but the post hoc test was proceeded

Table S10. Classification of PAHs via DTD-GC×GC-TOFMS. Target PAHs are marked italic and their areas are corrected by a purified air measurement. UFP-H (top), UFP-L (bottom).

UFP-H			
Compound/ Compound class	Retention Time 1 (s)	Retention Time 2 (s)	Peak Abundance (Area)
Parent-PAHs			
Phenanthrene	3229.84	3.649	924437625
Fluoranthene	3759.81	4.021	3352757901
Pyrene	3869.8	4.209	1685904171
5-Ring-PAH	4119.79	4.18	58440425
5-Ring-PAH	4154.79	4.281	192464711
5-Ring-PAH	4229.78	4.445	333702363
5-Ring-PAH	4314.78	4.552	3494257276
5-Ring-PAH	4324.77	4.556	727769405
Benz(a)anthracene	4399.77	4.539	952064678
5-Ring-PAH	4404.77	4.734	6430654103
Chrysene	4414.77	4.642	4844848166
5-Ring-PAH	4419.77	4.679	1107330242

4-Ring-PAH	4424.77	4.634	722086561
5-Ring-PAH	4514.76	4.63	282562936
5-Ring-PAH	4529.76	4.645	225078715
5-Ring-PAH	4579.76	4.725	390777923
4-Ring-PAH	4659.75	4.722	98356968
5-Ring-PAH	4784.74	4.955	84586368
5-Ring-PAH	4824.74	5.155	268174413
Benz(b)fluoranthene	4844.74	5.05	2115979302
Benz(k)fluoranthene	4849.74	5.156	4479045035
5-Ring-PAH	4849.74	5.156	4479045035
5-Ring-PAH	4889.74	5.165	1513635490
Benz(e)pyrene	4954.73	5.398	3309401173
Benz(a)pyrene	4974.73	5.412	4044799051
Perylene	5009.73	5.52	854562011
5-Ring-PAH	5024.73	5.168	139439001
5-Ring-PAH	5049.73	5.215	206737166
5-Ring-PAH	5059.73	5.295	639859268
5-Ring-PAH	5144.72	5.41	184671063
6-Ring-PAH	5269.71	5.704	319085960
6-Ring-PAH	5294.71	5.843	417174621
6-Ring-PAH	5309.71	5.977	547585433
5-Ring-PAH	5319.71	5.923	181809882
6-Ring-PAH	5329.71	6.099	1511632243
6-Ring-PAH	5339.71	6.173	584560527
Indeno(1,2,3,c,d)pyrene	5364.71	6.306	3815570110
Dibenz(a,h)anthracene	5379.71	6.26	247579289
6-Ring-PAH	5424.7	1.787	131253072
Benz(g,h,i)perylene	5464.7	2.183	12386155942
6-Ring-PAH	5509.7	2.507	6320293990
7-Ring-PAH	5769.68	4.675	175168025
7-Ring-PAH	5829.68	4.691	109790839
6-Ring-PAH	5854.68	4.732	461721061
6-Ring-PAH	5869.68	5.373	105179872
6-Ring-PAH	5884.67	4.996	267252697
6-Ring-PAH	5889.67	5.117	333031238
7-Ring-PAH	5954.67	5.88	1137637507
7-Ring-PAH	5969.67	5.993	284071850
7-Ring-PAH	5979.67	6.099	712429529
6-Ring-PAH	6004.67	6.254	156542434
6-Ring-PAH	6139.66	2.548	5345992340
Methyl-PAHs			
Meth-4-Ring-PAH	3959.8	4.027	99837227
Meth-4-Ring-PAH	4009.79	4.126	648485452
Meth-4-Ring-PAH	4054.79	4.226	204536762
Meth-4-Ring-PAH	4099.79	4.292	1435688064
Meth-5-Ring-PAH	5004.73	5.059	83900406

Meth-6-Ring-PAH	5584.69	2.74	2594445165
Meth-6-Ring-PAH	5599.69	2.786	1154146261
Meth-6-Ring-PAH	5674.69	3.466	254726699
Phenyl-PAHs			
Phenyl-3-Ring-PAH	4609.76	4.634	209528389
Phenyl-4-Ring-PAH	4929.74	5.078	152226137
Phenyl-4-Ring-PAH	4954.73	5.221	130711548
Phenyl-4-Ring-PAH	4984.73	5.227	172155651
Oxy-PAHs			
Oxy-4-Ring-PAH	4479.76	4.964	134753052
Oxy-5-Ring-PAH	4759.75	5.325	69234034
Oxy-5-Ring-PAH	4984.73	5.649	553850435
UFP-L			
Compound/ Compound class	Retention Time 1 (s)	Retention Time 2 (s)	Peak Abundance (Area)
Parent-PAHs			
Phenanthrene	3229.84	3.661	318086630
Pyrene	3869.8	4.225	63815016
Benz(a)anthracene	4399.77	4.584	114631437

Table S11. Targeted gas phase sample analyses of UFP-H and UFP-L taken in the adsorber tubes. The results are shown as mean ± standard deviation. For UFP-H: N= 3 For UFP-L: N=3

	UFP-H (ng/m^3)	**UFP-L (ng/m^3)**
Naphthalene	38 ± 7	57 ± 42
2-Methylnaphthalene	19 ± 6	20 ± 7
1-Methylnaphthalene	10 ± 2	10 ± 4
Biphenyl	8 ± 6	10 ± 10
1,2 Dimethylnaphthalene	137 ± 60	124 ± 61

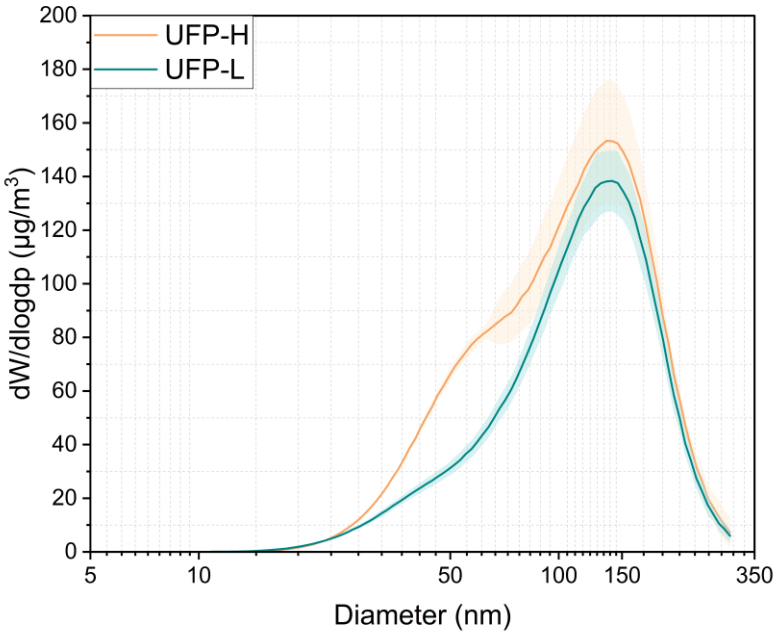

Figure S1. Exemplary mass size distribution of UFP- H and UFP-L. The shaded region is the standard deviation between the analyses.

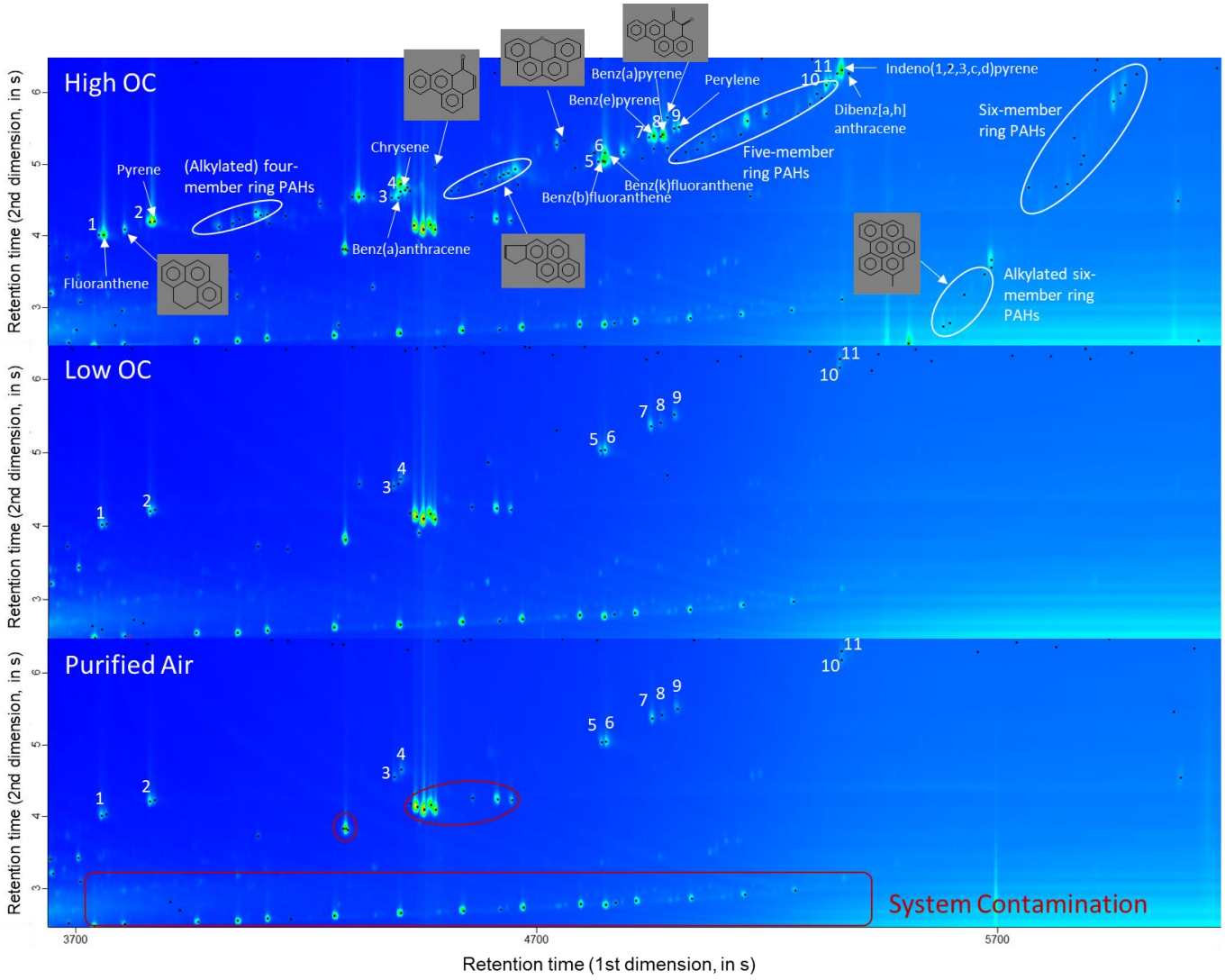

Figure S2. Section of the two-dimensional gas chromatograms of UFP-H, UFP-L and purified air showing the chromatographic region representative for PAHs. Potential structural formulas and compound classes are shown. Internal deuterated standards are numbered from 1 to 11. 1) Fluoranthene-d10, 2) Pyrene-d10, 3) Benz(a)anthracene-d10, 4) Chrysene-d10, 5) Benz(b)fluoranthene-d12, 6) Benz(k)fluoranthene-d12, 7) Benz(e)pyrene-d12, 8) Benz(a)pyrene-d12, 9) Pyrene-d12, 10) Indeno(1,2,3,c,d)pyrene-d12, 11) Dibenz(a,h)anthracene-d14. System contaminations are marked in red and are representative for all samples.

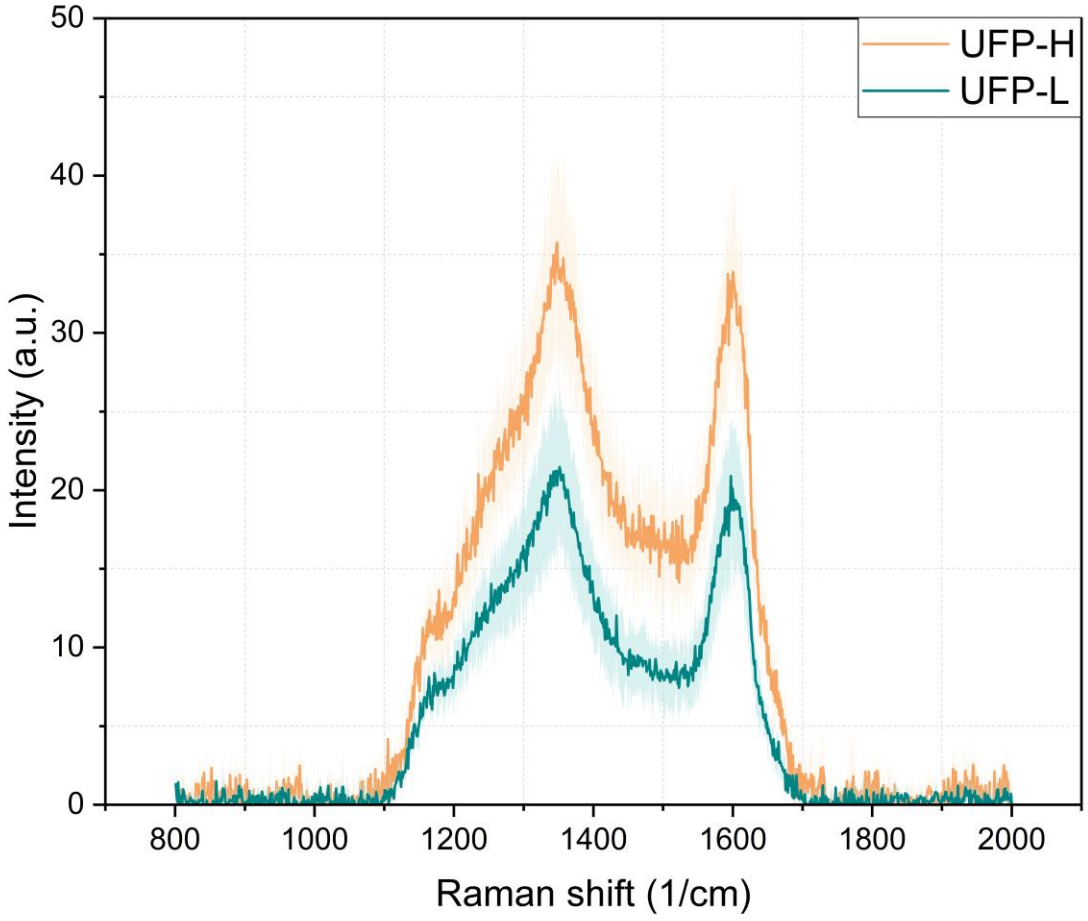

Figure S3. Raman spectrum for UFP- H and UFP-L for Group A. The shaded region is the standard deviation between the analyses.

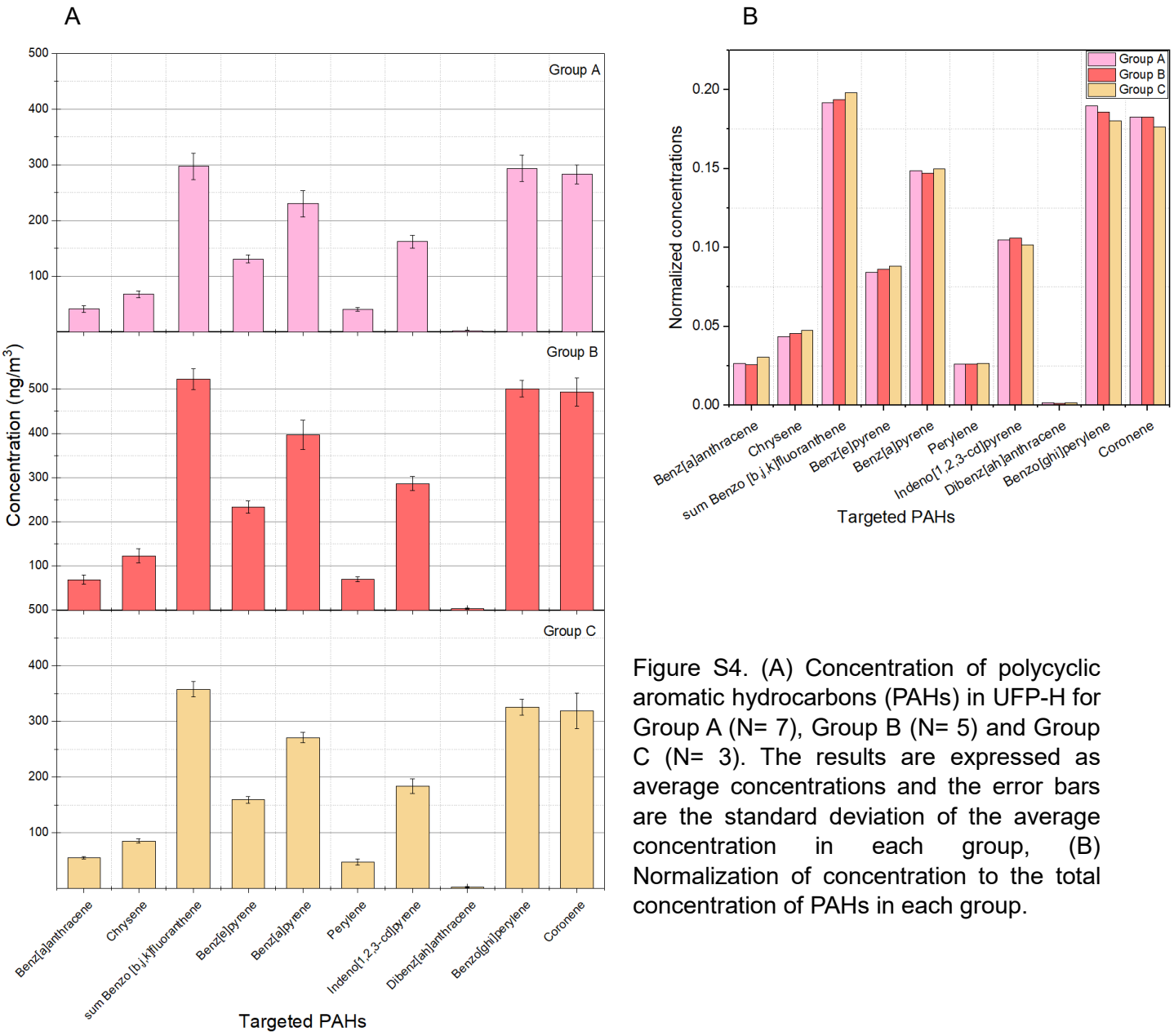

Figure S4. (A) Concentration of polycyclic aromatic hydrocarbons (PAHs) in UFP-H for Group A (N= 7), Group B (N= 5) and Group C (N= 3). The results are expressed as average concentrations and the error bars are the standard deviation of the average concentration in each group, (B) Normalization of concentration to the total concentration of PAHs in each group.

A

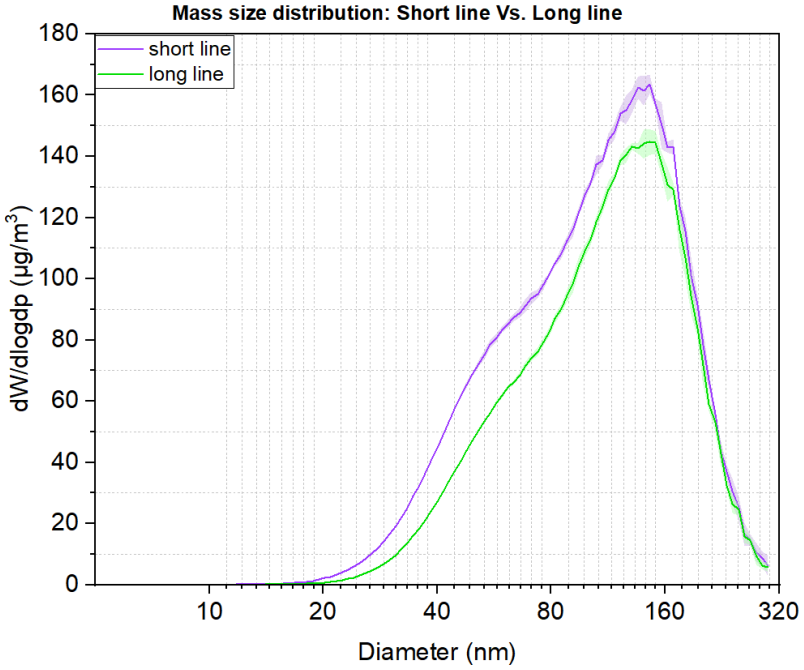

B

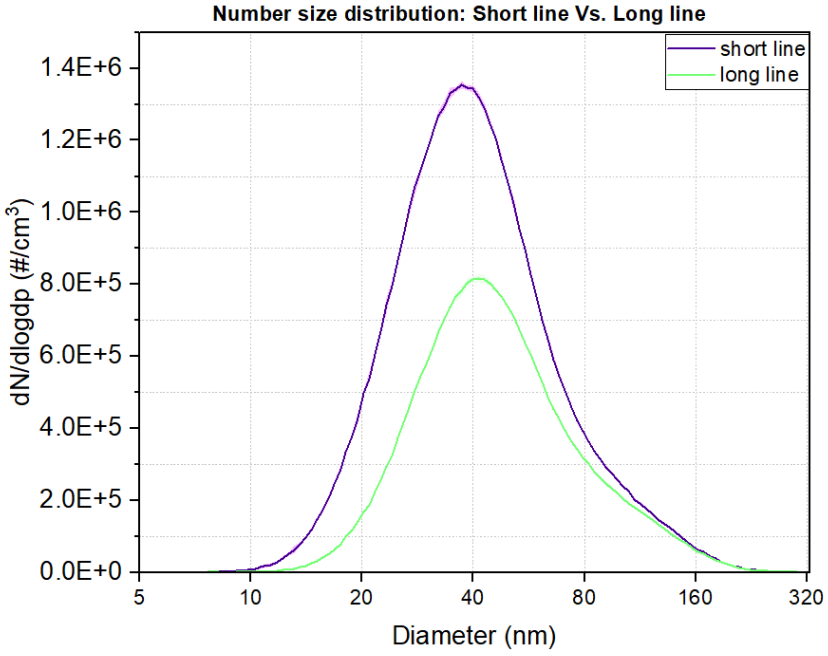

Figure S5. Particle losses on a short sampling line experiments (≈5 meters) and long sampling line experiments (≈20 meters) – (A) mass size distribution and (B) number size distribution. The shaded area represents the standard deviation of the number concentration (#/cm^3) in each size bins.